J Nanostruct 16(4): 5652-5662, Autumn 2026

RESEARCH PAPER

Green Synthesis of Zinc Oxide Nanostructures Using Medicinal Plants and Their Antibacterial Activity Against Multidrug-Resistant Uropathogenic Escherichia coli

*Thikra Ghaly AL-Timimi [1], Alaa Mohammed Khalil [2], Mazin Saleem Shakir [3], Baneen Ali Naji [4], Muslim M. M. Jassim [5], Osama A. Mohsein [6,7] **

[1] *General Directorate of Education, Najaf, Iraq*

[2] *Department of Pharmacognosy, College of Pharmacy, University of Kufa, Najaf, Iraq*

[3] *Department of Pharmacognosy, College of Pharmacy, University of Al-Ameed, Karbala, Iraq*

[4] *College of Pharmacy, Al-Zahraa University for Women, Karbala, Iraq*

[5] *College of Science, University of Cordoba, Najaf 54001, Iraq*

[6] *Department of Medical Laboratory Techniques, College of Health and Medical Techniques, Northern Technical University, Kirkuk, Iraq*

[7] *Thi-Qar Health Directorate, Al Habbobi Teaching Hospital, Thi-Qar, Iraq*

ARTICLE INFO

Article History:
Received 21 June 2026
Accepted 19 September 2026
Published 01 October 2026

Keywords:
Antibiofilm activity
Escherichia coli
Green synthesis
Multidrug resistance
Nanostructures
Zinc oxide

ABSTRACT

Multidrug-resistant uropathogenic *Escherichia coli* limits antibiotic effectiveness, encouraging green-synthesized zinc oxide nanostructures as promising alternative antibacterial agents. This study aimed to green-synthesize and characterize zinc oxide nanostructures using medicinal plant extracts and evaluate their antibacterial and antibiofilm activities against multidrug-resistant uropathogenic *Escherichia coli*. This laboratory-based experimental study was conducted from January to August 2026 using 150 urine samples. Uropathogenic *Escherichia coli* was isolated by standard culture and biochemical methods, and antimicrobial susceptibility was assessed by Kirby–Bauer testing. A medicinal plant extract was used for the green synthesis of ZnO nanostructures, which were characterized using UV–Vis, FT-IR, XRD, SEM, and TEM. Antibacterial activity was evaluated by agar well diffusion, while MIC and MBC were determined by broth microdilution. Antibiofilm activity was assessed using the microtiter-plate crystal violet assay. Among 150 urine samples, 108 (72.0%) were culture-positive, with *E. coli* accounting for 75.9% of isolates; 50 UPEC isolates were multidrug-resistant. Resistance was highest to ampicillin (84.1%), whereas imipenem showed 86.6% susceptibility. Green-synthesized ZnO exhibited a 369 nm absorption peak, hexagonal wurtzite structure, and 29.4±3.8-nm crystallite size. Antibacterial activity increased concentration-dependently, reaching a 20.9±2.7-mm inhibition zone at 200 µg/mL. Most isolates showed MIC and MBC values of 100 and 200 µg/mL, respectively. Biofilm inhibition reached 62.4±9.8% at 200 µg/mL. In conclusion, green-synthesized ZnO nanostructures demonstrated concentration-dependent antibacterial and antibiofilm activity against multidrug-resistant UPEC isolates. Their favorable physicochemical characteristics and relatively low inhibitory concentrations support their potential as alternative antimicrobial agents. Further toxicity, biocompatibility, mechanistic, and in vivo studies are required before clinical application.

How to cite this article
Ghaly AL-Timimi T., Mohammed Khalil A., Saleem Shakir M. et al. Green Synthesis of Zinc Oxide Nanostructures Using Medicinal Plants and Their Antibacterial Activity Against Multidrug-Resistant Uropathogenic Escherichia coli. J Nanostruct, 2026; 16(4):5652-5662. DOI: 10.22052/JNS.2026.04.095

* *Corresponding Author Email: osamaakram889@gmail.com*

This work is licensed under the Creative Commons Attribution 4.0 International License.
To view a copy of this license, visit http://creativecommons.org/licenses/by/4.0/.

INTRODUCTION

Urinary tract infections (UTIs) are one of the most common bacterial infections in clinical practice and are a significant burden on the healthcare system due to their high incidence, the high risk of recurrence, and the need for antimicrobial therapy. Uropathogenic *Escherichia coli* (UPEC) is the most common cause of both community- and HAI-associated UTIs and has unique virulence determinants that enable UPEC to colonize, persist, and invade the urinary tract [1, 2]. These include adhesins, fimbriae, iron-acquisition mechanisms, toxins, motility-associated factors, and intracellular survival and biofilm formation mechanisms [2, 3]. Biofilm formation is pertinent for the ability of bacteria to persist in the body, to cause recurrent infection, and to become less susceptible to antimicrobials [3, 4].

Multidrug-resistant (MDR) UPEC strains have emerged and spread, making infection management more difficult. Therapeutic options are limited, and the risk of treatment failure and recurrent disease is high because of resistance to β-lactams, fluoroquinolones, aminoglycosides, and other common antimicrobial classes used in treatment [5, 6]. UPEC resistance is further complicated by extended-spectrum β-lactamase production, changes in the antimicrobial target, decreased membrane permeability, active efflux, horizontal acquisition of resistance determinants, and biofilm protection [7]. The combination of virulence, biofilm production, and multidrug resistance highlights the importance of developing alternative approaches that target new mechanisms of action rather than traditional antibiotics [8].

Nanotechnology has therefore gained much attention as an alternative route for the formulation of novel antimicrobial materials. The zinc oxide nanoparticles and nanostructures (ZnO-NPs) are among the most promising metal oxide nanomaterials due to their physicochemical stability, low cost, and high surface-to-volume ratio, as well as their wide antimicrobial activity [9]. The antibacterial action has been suggested to be due to a combination of mechanisms such as the production of ROS, release of Zn^{2+} ions, disruption of bacterial membrane integrity, alteration of membrane permeability, oxidative damage to cellular components, and disruption of essential metabolic pathways [10]. Combined use of several different antibacterial mechanisms might be beneficial in the treatment of bacteria with "classic" drug-resistant phenotypes.

The traditional physical and chemical methods for the production of nanostructures of ZnO can consume significant amounts of energy, involve harsh reaction conditions or chemical reducing and stabilizing agents, which can leave unwanted residues. The green synthesis approach based on biological resources has thus become an environmentally friendly technology [11, 12]. Medicinal plant extracts contain a variety of phytochemicals such as polyphenols, flavonoids, terpenoids, alkaloids, proteins, sugars, and organic acids, which can participate in the formation, stabilization, and functionalization of nanoparticles on the surface [13]. Typically, plant-mediated synthesis is simple, inexpensive, and can be easily integrated with the reduction of hazardous chemicals used, and the phytochemical coating of biogenic particles can alter the biological properties of the particles [13, 14].

In recent years, the use of plants to synthesize ZnO nanostructures has been proven to be effective for plants such as Scoparia dulcis, Cocos nucifera, Viscum album, Pluchea indica, Mentha piperita, and Allium cepa [15]. These investigations have reported the antimicrobial activity of these nanoscale structures of ZnO crystallized against several Gram-positive and Gram-negative pathogens. Importantly, ZnO nanoparticles synthesized using Mentha piperita exhibited activity against antimicrobial-resistant microorganisms causing UTIs [16, 17], and other green-synthesized ZnO nanoparticles have been reported to exhibit inhibitory effects against MDR clinical bacteria [18]. Plant-derived ZnO nanoparticles also showed activity against *E. coli,* indicating their potential as an alternative antibacterial material [19].

However, there are significant differences in the antimicrobial activity depending on the botanical origin, phytochemical content, method of preparation, particle size, shape, surface properties, concentration, and phenotype of the bacteria. Moreover, there is comparatively limited evidence directly targeting clinically relevant MDR UPEC isolates using plant-mediated ZnO nanostructures. Hence, a comparison of green-synthesized ZnO nanostructures with the resistant uropathogenic *E. coli* could be a useful indication to determine the sustainability of the prepared nanotech material for its possible use as an antimicrobial material. In the present study, zinc oxide nanostructures were synthesized and characterized using medicinal plant extracts, and their antibacterial activity

CC BY

against multidrug-resistant UPEC was evaluated.

MATERIALS AND METHODS

Study Design and Sample Collection

This laboratory-based experimental study was conducted from January to August 2026 to evaluate the antibacterial activity of green-synthesized zinc oxide (ZnO) nanostructures against multidrug-resistant uropathogenic *Escherichia coli* (UPEC). A total of 150 midstream urine samples were collected from patients with a clinical diagnosis of urinary tract infection (UTI) attending outpatient clinics and microbiology laboratories. Urine samples were collected in sterile containers and promptly transported to the laboratory for microbiological analysis.

Isolation and Identification of Bacterial Isolates

Urine samples were cultured on CLED (cystine–lactose–electrolyte-deficient) agar and MacConkey agar plates and incubated aerobically at 37°C for 24 hours. Significant bacteriuria was defined as a bacterial count of $\geq 10^5$ CFU/mL. *Escherichia coli* isolates were identified based on colony morphology, Gram staining, and standard biochemical tests, including triple sugar iron (TSI) agar, urease, indole production, and motility tests.

Antibiotic Susceptibility Testing

Antimicrobial susceptibility testing was performed using the Kirby–Bauer disk diffusion method on Mueller–Hinton agar, following the guidelines of the Clinical and Laboratory Standards Institute (CLSI). Antibiotics tested were ampicillin, cefotaxime, ceftazidime, ciprofloxacin, gentamicin, nitrofurantoin, and imipenem. Isolates resistant to at least three different antimicrobial classes were considered multidrug-resistant (MDR).

Preparation of Medicinal Plant Extract

Fresh medicinal plant leaves were thoroughly washed with distilled water and then air-dried at room temperature. Dried plant material was finely ground using an electric grinder. The powdered material (about 20 g) was mixed with 200 mL of distilled water and heated at 60°C for 30 minutes. The extract was filtered through Whatman No. 1 filter paper and stored at 4°C for further use.

Green Synthesis of Zinc Oxide Nanostructures

50 mL of plant extract was added to 50 mL of zinc acetate dihydrate solution (0.1 M), and the mixture was stirred continuously at 70°C till the pH of the mixture reached 10 by dropwise addition of sodium hydroxide solution. The formation of ZnO nanostructures was evidenced by the appearance of a pale white precipitate. The precipitate was centrifuged at 10,000 rpm for 15 minutes, washed with distilled water and ethanol many times, dried at 80°C overnight, and then calcined at 400°C for 2 hours.

Characterization of Synthesized ZnO Nanostructures

The synthesized zinc oxide (ZnO) nanostructures

Table 1. Distribution of urine culture results and uropathogenic *Escherichia coli* isolates among the examined clinical samples.

Parameter	NO. (n)	Percentage (%)
Total urine samples	150	100
Positive bacterial culture	108	72.0
Negative bacterial culture	42	28.0
E. coli isolates	82	75.9
Non-*E. coli* isolates	26	24.1
MDR UPEC isolates selected for testing	50	61.0

CC BY

were characterized using various analytical techniques. UV–Visible (UV–Vis) spectroscopy was employed to determine the optical absorption characteristics of the samples. Fourier-transform infrared (FT-IR) spectroscopy was used to identify the functional groups associated with the plant-derived compounds involved in nanoparticle formation and stabilization. X-ray diffraction (XRD) analysis was performed to determine the crystalline structure and estimate the average crystallite size of the ZnO nanostructures. Scanning electron microscopy (SEM) and transmission electron microscopy (TEM) were used to examine the surface morphology, particle shape, and size distribution of the synthesized nanostructures.

Evaluation of Antibacterial Activity

The antibacterial activity of the synthesized zinc oxide (ZnO) nanostructures was evaluated against multidrug-resistant uropathogenic *Escherichia coli* (MDR UPEC) isolates using the agar well diffusion method. ZnO nanoparticle suspensions were prepared at concentrations of 25, 50, 100, and 200 µg/mL. Mueller–Hinton agar plates were inoculated with standardized bacterial suspensions adjusted to the 0.5 McFarland turbidity standard. Wells were aseptically prepared in the inoculated agar, and the ZnO nanoparticle suspensions were added to the wells. Following incubation at 37°C for 24 h, the diameters of the inhibition zones were measured in millimeters.

Determination of Minimum Inhibitory Concentration (MIC) and Minimum Bactericidal Concentration (MBC)

The minimum inhibitory concentration (MIC) and minimum bactericidal concentration (MBC) of the synthesized ZnO nanostructures were determined using the broth microdilution method. Standardized bacterial suspensions were added to broth containing serial dilutions of the ZnO nanostructures. Appropriate growth and sterility controls were included. Following incubation under the specified conditions, the MIC was defined as the lowest concentration of ZnO nanostructures that prevented visible bacterial growth. To determine the MBC, aliquots from wells showing no visible growth were subcultured onto suitable agar plates. The MBC was defined as the lowest concentration that resulted in no detectable bacterial growth on the agar following incubation.

Biofilm Inhibition Assay

The antibiofilm activity of the synthesized zinc oxide (ZnO) nanostructures was evaluated using the crystal violet staining method in 96-well microtiter plates. Multidrug-resistant uropathogenic *Escherichia coli* (MDR UPEC) isolates were incubated in the presence of different concentrations of ZnO nanostructures for 24 h. Following incubation, the biofilms were stained with crystal violet, and the attached biomass was quantified by measuring the absorbance at 570 nm using a microplate reader. Biofilm inhibition was expressed as a percentage relative to the untreated control.

Statistical Approval

Statistical analyses were performed using SPSS software, version 26 (IBM Corp., Armonk, NY, USA). Quantitative variables were expressed as mean ± standard deviation (SD), whereas categorical variables were presented as frequencies and percentages. Differences in antibacterial activity among the different ZnO nanostructure concentrations were assessed using one-way analysis of variance (ANOVA), followed by Tukey's post hoc test for pairwise comparisons.

The chi-square test was used to analyze categorical comparisons. A p-value of of less than

Table 2. Distribution of Antimicrobial Susceptibility Profiles Among Clinical Uropathogenic *Escherichia coli* (UPEC) Isolates Against Seven Antibiotics.

Antibiotic	Resistant No. (%)	Intermediate No. (%)	Sensitive No. (%)
Ampicillin	69 (84.1)	4 (4.9)	9 (11.0)
Cefotaxime	58 (70.7)	6 (7.3)	18 (22.0)
Ceftazidime	55 (67.1)	7 (8.5)	20 (24.4)
Ciprofloxacin	51 (62.2)	5 (6.1)	26 (31.7)
Gentamicin	37 (45.1)	8 (9.8)	37 (45.1)
Nitrofurantoin	22 (26.8)	5 (6.1)	55 (67.1)
Imipenem	8 (9.8)	3 (3.7)	71 (86.6)

0.05 was considered statistically significant.

Ethical Approval

The study protocol was approved by the relevant institutional ethics committee, and informed consent was obtained from all participants before sample collection. Ethical principles and laboratory biosafety procedures were followed throughout the study.

RESULTS AND DISCUSSION

Frequency of culture positivity, bacterial isolates, and multidrug-resistant UPEC selected for subsequent antibacterial testing.

The 108 urine samples that were cultured were positive for bacteria, while 42 (28.0%) were negative for bacteria. Among the 108 positive cultures, the most common bacterial isolate was *Escherichia coli* (82, 75.9%), and the non-E. coli uropathogens were (26, 24.1%). Of the 82 UPEC isolates, 50 (61.0%) were multidrug-resistant and chosen for further testing of the antimicrobial and anti-biofilm properties of the synthesized ZnO nanostructures, as shown in Table 1.

Distribution of resistant, intermediate, and susceptible phenotypes among 82 clinical UPEC isolates tested against seven antibiotics

As shown in Table 2, the study of antimicrobial susceptibility showed the highest resistance to ampicillin (84.1%), followed by cefotaxime (70.7%), ceftazidime (67.1%), and ciprofloxacin (62.2%). The same proportion of resistant (45.1%) and susceptible (45.1%) isolates was seen for gentamicin. Comparatively lower resistance was seen towards nitrofurantoin (26.8%) and imipenem (9.8%). There was substantial variation in antimicrobial susceptibility, with imipenem

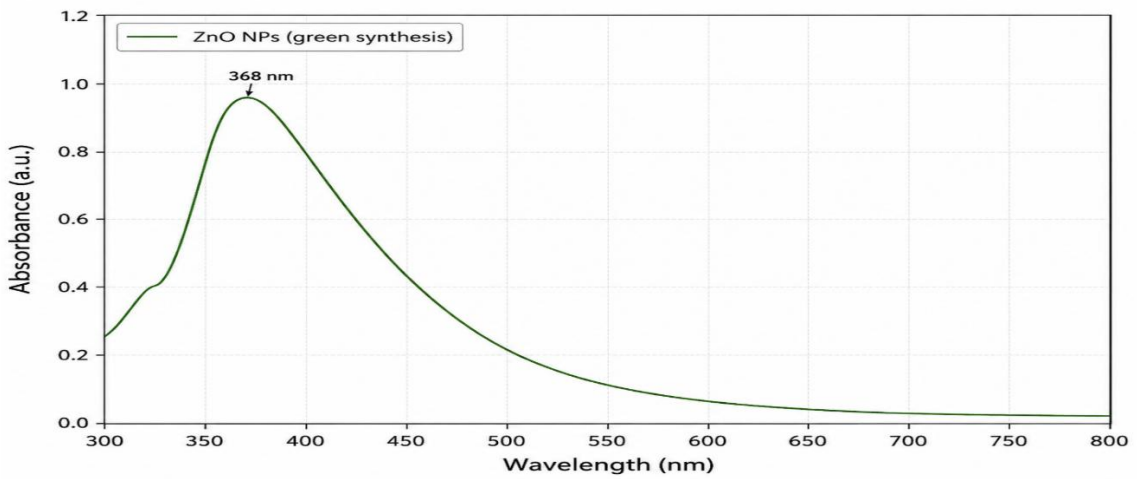


Fig. 1. UV–Visible absorption spectrum of green-synthesized ZnO nanostructures.

Table 3. Physicochemical Characterization of Green-Synthesized Zinc Oxide Nanostructures by Spectroscopic, Microscopic, and Crystallographic Techniques.

Characterization parameter	Result
Plant extract appearance	Light brown aqueous extract
Color change after ZnO formation	Pale yellow to milky white
UV–Visible absorption peak	369 nm
FT-IR major functional groups	O–H, C=O, C–O, Zn–O
XRD crystalline structure	Hexagonal wurtzite ZnO
Mean crystallite size	29.4 ± 3.8 nm
SEM morphology	Spherical to short rod-like particles
Zeta potential	−25.7 ± 2.9 mV
Polydispersity index	0.33 ± 0.05

showing the highest activity (86.6% susceptible), followed by nitrofurantoin (67.1% susceptible).

Optical, structural, morphological, surface-charge, and particle-distribution characteristics of ZnO nanostructures

As shown in Table 3, the green-synthesized ZnO nanostructures exhibited characteristic optical, structural, morphological, and physicochemical properties. The initial colour change from pale yellow to milky white suggested successful synthesis. UV–Visible spectroscopy revealed a characteristic absorption peak at 368 nm (Fig. 1), while FT-IR analysis identified O–H, C=O, C–O, and Zn–O functional groups, as shown in (Fig. 4). XRD analysis confirmed the hexagonal wurtzite crystalline structure, with an average crystallite size of 29.4 ± 3.8 nm (Fig. 2). SEM examination revealed predominantly spherical to short rod-like particles Fig. 3 (a-c). As shown in Fig. 3(d–f), TEM images revealed the interplanar spacing of 0.281 nm, corresponding to the (100) plane, further confirms the nanorod-like structure of ZnO nanostructures. The synthesized nanostructures exhibited a zeta potential of −25.7 ± 2.9 mV and a polydispersity index (PDI) of 0.33 ± 0.05.

Comparison of inhibition-zone diameters produced by increasing ZnO concentrations, plant extract, and positive antibiotic control

As shown in Table 4, the green-synthesized ZnO nanostructures exhibited a concentration-dependent enhanced antibacterial activity against MDR UPEC isolates. The mean inhibition zone increased from 9.6 ± 1.5 mm at 25 µg/mL to 12.8 ± 1.9 mm at 50 µg/mL, and 16.7 ± 2.3 mm at 100 µg/mL, and 20.9 ± 2.7 mm at 200 µg/mL ($P<0.001$). The plant extract alone produced an inhibition zone of 7.4 ± 1.2 mm, which was not statistically significant ($P = 0.081$). Notably, ZnO nanostructures at 200 µg/mL produced a larger mean inhibition zone than the positive antibiotic control (19.2 ± 3.0 mm).

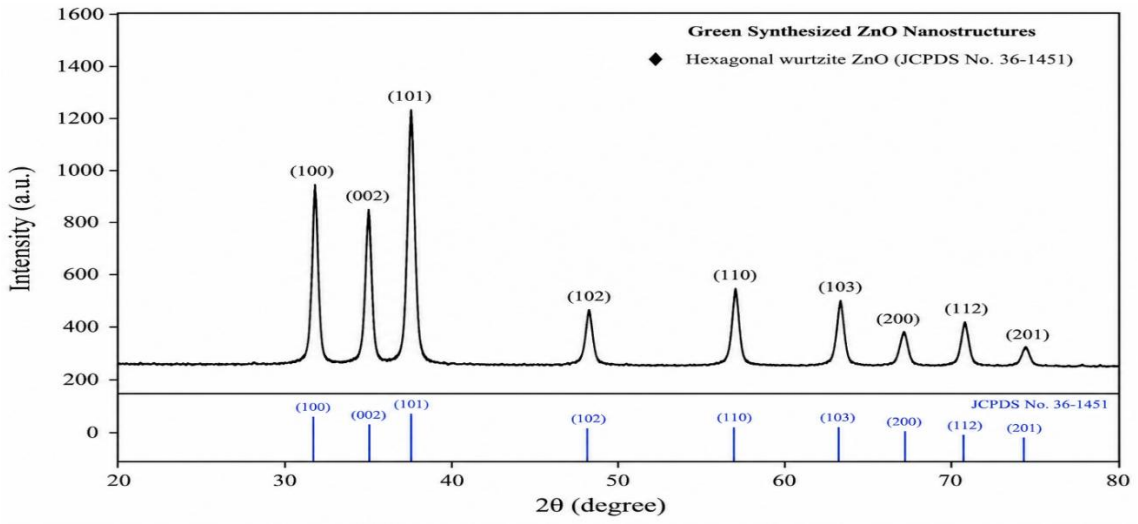


Fig. 2. X-ray diffraction (XRD) pattern of green-synthesized ZnO nanostructures.

Table 4. Comparison of the Antibacterial Activity of Green-Synthesized Zinc Oxide Nanostructures, Plant Extract, and Positive Antibiotic Control Against Multidrug-Resistant Uropathogenic *Escherichia coli*.

Treatment	Zone of inhibition, mm Mean ± SD	p-value
Plant extract only	7.4 ± 1.2	0.081
ZnO at 25 µg/mL concentration	9.6 ± 1.5	0.046
ZnO at 50 µg/mL concentration	12.8 ± 1.9	0.011
ZnO at 100 µg/mL concentration	16.7 ± 2.3	<0.001
ZnO at 200 µg/mL concentration	20.9 ± 2.7	<0.001
Positive control antibiotic	19.2 ± 3.0	<0.001

CC BY

Distribution of MIC and MBC endpoints among 50 multidrug-resistant UPEC isolates exposed to increasing ZnO concentrations

As summarized in Table 5, among the 50 multidrug-resistant (MDR) UPEC isolates, the most frequently observed minimum inhibitory concentration (MIC) was 100 µg/mL, detected in 28 isolates (56.0%), followed by 200 µg/mL in 15 isolates (30.0%) and 50 µg/mL in 7 isolates (14.0%). Higher concentrations were generally required to achieve bactericidal activity. The most frequent minimum bactericidal concentration (MBC) was 200 µg/mL, observed in 31 isolates (62.0%), followed by 100 µg/mL in 10 isolates (20.0%) and 400 µg/mL in 9 isolates (18.0%). Overall, the higher MBC values compared with MIC values indicate that greater concentrations of ZnO nanostructures were generally required to achieve bactericidal effects than to inhibit bacterial growth.

Comparison of biofilm inhibition following treatment with increasing ZnO concentrations, plant extract, and positive antibiotic control

Biofilm inhibition increased progressively with increasing ZnO concentration, reaching 30.6 ± 7.5% at 50 µg/mL (P = 0.026), 46.9 ± 8.7% at 100 µg/mL (P = 0.003), and 62.4 ± 9.8% at 200 µg/mL (P < 0.001). The plant extract alone showed a lower inhibition rate of 17.9 ± 5.8%, which was not statistically significant (P = 0.073). Notably, ZnO at 200 µg/mL achieved greater biofilm inhibition than the positive antibiotic control (51.6 ± 10.4%; P = 0.002), as presented in Table 6.

In the present study, bacterial growth was detected in 108 of 150 urine samples (72.0%), indicating a high prevalence of culture-positive urinary tract infections (UTIs) in the study population. Among the culture-positive isolates, *Escherichia coli* was the predominant species,

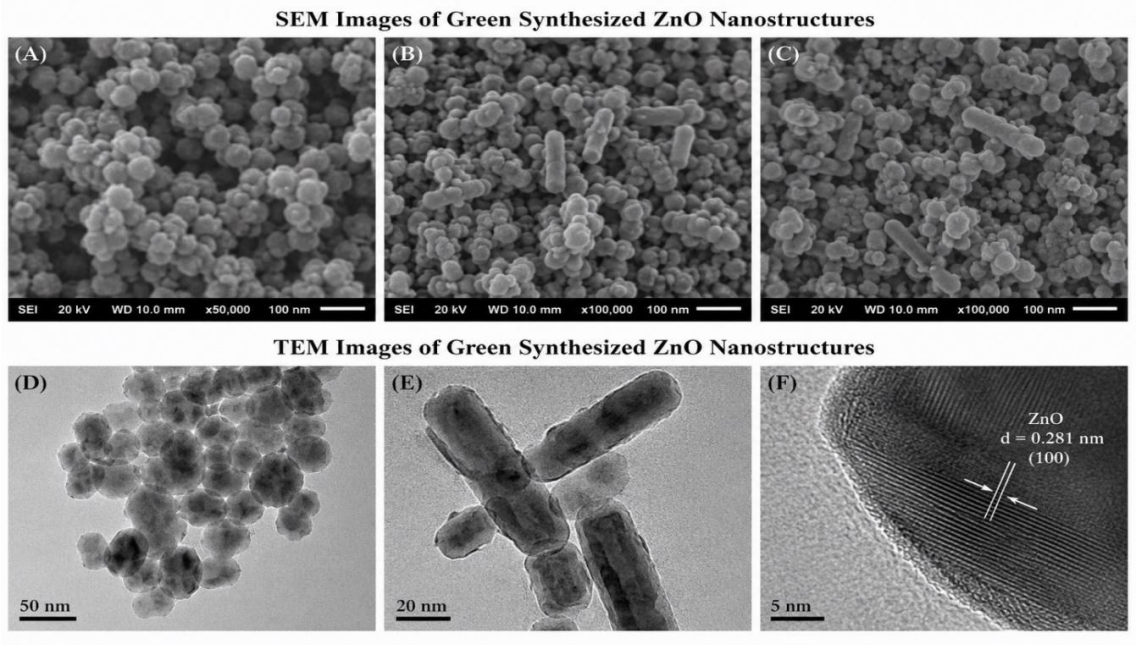


Fig. 3. SEM (a–c) and TEM (d–f) graphs showing the morphology of green-synthesized ZnO nanostructures.

Table 5. Minimum Inhibitory and Bactericidal Concentrations of Green-Synthesized ZnO Nanostructures Against Multidrug-Resistant Uropathogenic *Escherichia coli* isoltes.

Concentration (µg/mL)	MIC No. (%)	MBC No. (%)
50	7 (14.0)	0 (0.0)
100	28 (56.0)	10 (20.0)
200	15 (30.0)	31 (62.0)
400	0 (0.0)	9 (18.0)
Total	50 (100)	50 (100)

CC BY

accounting for 75.9% of the isolates. This finding is consistent with Assafi et al. [20], who identified *E. coli* as a major causative agent of UTIs and reported a considerable prevalence of multidrug resistance (MDR) among urinary isolates. Similarly, Jalil and Al Atbee [21] reported a high prevalence of MDR *E. coli* among patients with UTIs. Alfuraizi et al. [22] also highlighted the continued importance of uropathogenic *E. coli* (UPEC) as a major urinary pathogen associated with substantial antimicrobial resistance. Differences in prevalence rates across studies may be attributable to variations in study populations, geographical locations, previous antibiotic exposure, patient age, specimen collection methods, and healthcare-associated risk factors. The antimicrobial susceptibility profile reported in this study also highlights the clinical problem associated with UPEC. The highest resistance (84.1%) was to ampicillin, followed by cefotaxime (70.7%), ceftazidime (67.1%), and ciprofloxacin (62.2%). In the same way, Eezzeldin et al. [23] also found that multidrug resistance was high for UPEC against some of the antimicrobial agents commonly used. Most importantly, in the present study, imipenem was the most active antibiotic, with 86.6% of the isolates being susceptible. However, Al-Mayahie et al. [24] reported the presence of carbapenemase genes in Iraqi UPEC, suggesting the emergence of resistance to last-line antibiotics. The high resistance levels against beta-lactams could be due to the selection pressure exerted by the use of these antibiotics and the spread of plasmid-mediated beta-lactamases; higher susceptibility levels against imipenem could be a reflection of the comparatively limited use of this antibiotic.

The physicochemical characterization results confirmed the successful formation of plant-mediated nanostructures of ZnO. The characteristic optical behavior for green synthesized ZnO nanoparticles [25] was found to be compatible with the UV–visible absorption maximum at 368

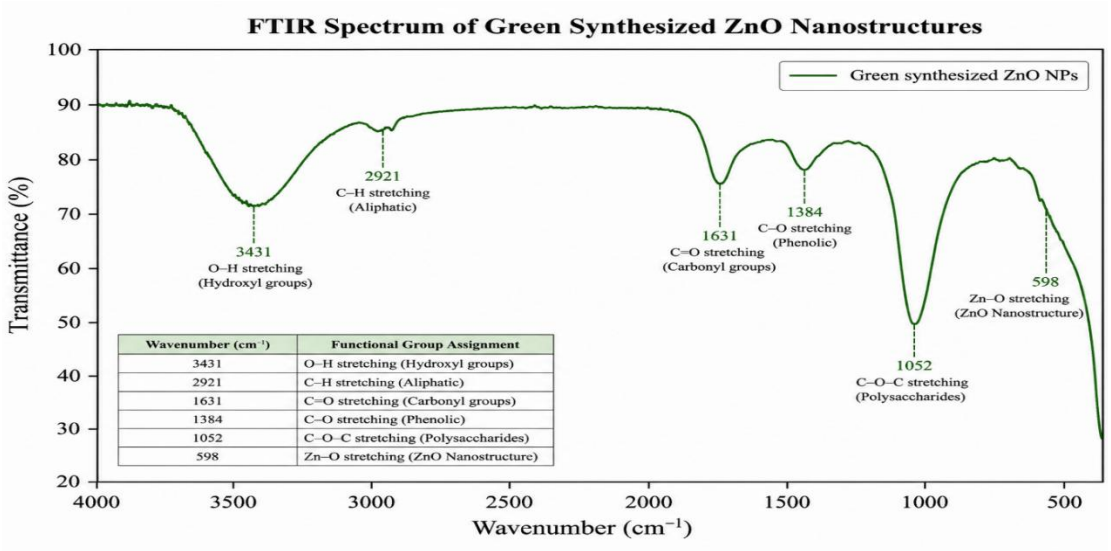


Fig. 4. FT-IR spectrum of green synthesized ZnO nanostructures.

Table 6. Antibiofilm Activity of Green-Synthesized ZnO Nanostructures at Different Concentrations Against Multidrug-Resistant Uropathogenic *Escherichia coli*.

Treatment	Biofilm inhibition (%) (Mean ± SD)	p-value
Plant extract only	17.9 ± 5.8	0.073
ZnO 50 µg/mL	30.6 ± 7.5	0.026
ZnO 100 µg/mL	46.9 ± 8.7	0.003
ZnO 200 µg/mL	62.4 ± 9.8	<0.001
Positive control antibiotic	51.6 ± 10.4	0.002

CC BY

nm. A similar kind of spectra and crystal structure wurtzite hexagonal have been reported for plant-mediated preparation of ZnO [26]. Furthermore, the mean crystallite size range (29.4 ± 3.8 nm) and the spherical to short rod-like shape of the crystals are similar to the nano-scale range (18–35 nm) observed in some of the more recent phytochemical synthesis studies [27]. But, Dey et al. [28] demonstrated that nanoparticle size alone does not necessarily determine biological activity, as particles smaller than 50 nm do not invariably exhibit strong antibacterial effects. In the present study, the zeta potential of −25.7 ± 2.9 mV suggested moderate colloidal stability, consistent with the negative surface potentials reported for biosynthesized ZnO-based nanomaterials [29].

One of the key findings of this study was the concentration-dependent antibacterial activity of the green-synthesized ZnO nanostructures against multidrug-resistant (MDR) UPEC isolates. The inhibition zone increased progressively from 9.6 ± 1.5 mm at 25 µg/mL to 20.9 ± 2.7 mm at 200 µg/mL. ZnO nanoparticles may damage bacterial membranes through several mechanisms, including direct interactions with the membrane, the release of Zn^{2+} ions, and the generation of reactive oxygen species (ROS) [30]. Likewise, other biosynthesized ZnO formulations have demonstrated increased antibacterial activity against bacterial species such as *E. coli* at higher nanoparticle concentrations [31].

Increased contact with bacterial surfaces, enhanced Zn^{2+} release, and elevated oxidative stress may contribute to the greater antibacterial activity observed at higher ZnO concentrations. Experimental studies have shown that ZnO exposure can induce ROS generation, lipid peroxidation, membrane disruption, protein dysfunction, and DNA damage in bacteria [32]. These mechanisms may act simultaneously and are particularly relevant against MDR organisms, as they differ from the target-specific mechanisms of conventional antibiotics. Moreover, several studies have demonstrated the antibiofilm activity of green-synthesized ZnO at relatively low concentrations, although its efficacy depends on the synthesis method and bacterial species [33].

The MIC results further support the antibacterial activity of the synthesized nanostructures. Among the 50 MDR UPEC isolates, 56.0% exhibited an MIC of 100 µg/mL, while 30.0% showed an MIC of 200 µg/mL. Regarding MBC, 62.0% and 18.0% of isolates required concentrations of 200 and 400 µg/mL, respectively. These values were substantially lower than the MIC and MBC values of approximately 3.2 and 3.9 mg/mL, respectively, reported by Abu-Gharbia et al. [34] for biosynthesized ZnO nanoparticles against UPEC. The present findings are more consistent with those of Elekhnawy et al. [35], who reported MIC values ranging from 32 to 128 µg/mL for clinical *Proteus mirabilis* isolates. These differences may be attributed to variations in bacterial species and strains, nanoparticle size and shape, phytochemical surface coating, nanoparticle aggregation, Zn^{2+} dissolution, inoculum density, and experimental methodology.

The present study also demonstrated substantial antibiofilm activity. Biofilm inhibition was concentration-dependent, increasing from 30.6% at 50 µg/mL to 62.4% at 200 µg/mL. Similarly, Hasan et al. [36] reported that ZnO nanoparticles inhibited biofilm formation by UPEC. Shakerdarabad et al. [37] also demonstrated significant antibacterial and antibiofilm activities of green-synthesized ZnO nanoparticles, further supporting their potential to disrupt bacterial communities. In another study, Abdelghafar et al. [38] reported that ZnO nanoparticles inhibited biomass formation and enhanced antibacterial activity against *Staphylococcus aureus*. These findings across different bacterial species suggest that the ability to interfere with biofilm development may be a broader biological property of ZnO nanomaterials rather than one limited to UPEC.

Mechanistically, the antibiofilm effects of ZnO nanostructures may involve the inhibition of initial bacterial adhesion, disruption of membrane integrity, suppression of extracellular polymeric substance production, induction of oxidative stress, and interference with cellular pathways associated with biofilm formation. Importantly, the biological activity of ZnO nanoparticles also depends on their morphology. Studies investigating antibacterial activity, bacterial gene expression, flagellar assembly, and biofilm-associated pathways have shown that nanoparticle morphology can influence these processes [39]. This may help explain the variations in antibacterial activity reported in the literature. Overall, the present findings demonstrate the antibacterial and antibiofilm potential of medicinal plant-mediated ZnO nanostructures against MDR UPEC. However, differences among published studies highlight the need to standardize nanoparticle composition and physicochemical properties. Further investigations

CC BY

into toxicity, biocompatibility, pharmacological behavior, and in vivo efficacy are also necessary before potential therapeutic applications can be considered.

CONCLUSION

Multidrug-resistant uropathogenic *Escherichia coli* was effectively inhibited by a green-synthesized ZnO nanostructure due to its significant antibacterial and antibiofilm activity. The nanostructures had good physicochemical properties, such as a nanocrystallite size and a well-defined hexagonal wurtzite structure. They exhibited antibacterial activity in a concentration-dependent manner, with the highest inhibition at 200 µg/mL, and relatively low MIC and MBC values, showing good growth suppression. The formation of biofilm was also significantly restricted with the help of ZnO nanostructures, thus supporting their potential activity against the planktonic as well as the biofilm-associated UPEC. Based on the results presented in this study, it can be concluded that the plant-mediated ZnO nanostructures could be a potential alternative and/or complementary antimicrobial approach to combat multidrug-resistant UPEC. However, to prove their potential for clinical application, further mechanistic studies, cytotoxicity and biocompatibility evaluation, animal studies, and standard in vivo evaluation must be performed.

CONFLICT OF INTEREST

The authors declare that there is no conflict of interests regarding the publication of this manuscript.

REFERENCES

1. Kadhum DA, Al-Qaisi SK, Mohammad SQ, Jalil IS. Assessing the genetic basis of antibiotic resistance in Escherichia coli through advanced electrophoretic and PCR techniques. Regulatory Mechanisms in Biosystems. 2025;33(1):e25036.
2. Torres-Puig S, García V, Stærk K, Andersen TE, Møller-Jensen J, Olsen JE, et al. "Omics" Technologies - What Have They Told Us About Uropathogenic Escherichia coli Fitness and Virulence During Urinary Tract Infection? Frontiers in Cellular and Infection Microbiology. 2022;12.
3. Zhang T, Ray S, Melican K, Richter-Dahlfors A. The maturation of native uropathogenic Escherichia coli biofilms seen through a non-interventional lens. Biofilm. 2024;8:100212.
4. Malik AW, Mohsen SM, Mohsen AK, Mohammad SQ, Mohsein OA. Bacterial strains isolated from sinusitis infections and their drug resistance profiles in Nasiriyah (Iraq). Regulatory Mechanisms in Biosystems. 2025;16(2):e25049.
5. Simoni A, Schwartz L, Junquera GY, Ching CB, Spencer JD. Current and emerging strategies to curb antibiotic-resistant urinary tract infections. Nature Reviews Urology. 2024;21(12):707-722.
6. Abo-alella D, Abdelmoniem W, Tantawy E, Asaad A. Biofilm-producing and carbapenems-resistant Escherichia coli nosocomial uropathogens: a cross-sectional study. Int Microbiol. 2024;27(6):1633-1640.
7. Choi N, Choi E, Cho Y-J, Kim MJ, Choi HW, Lee E-J. A shared mechanism of multidrug resistance in laboratory-evolved uropathogenic Escherichia coli. Virulence. 2024;15(1).
8. Okaiyeto K, Gigliobianco MR, Di Martino P. Biogenic Zinc Oxide Nanoparticles as a Promising Antibacterial Agent: Synthesis and Characterization. Int J Mol Sci. 2024;25(17):9500.
9. Essa SH, Mohammad SQ, Kadhum DA, Jalil IS. Effectiveness of silver nanoparticles as antibacterial agents with natural wound healing cream with extracted Aloe vera gel. Regulatory Mechanisms in Biosystems. 2024;15(4):821-825.
10. Xu J, Huang Y, Zhu S, Abbes N, Jing X, Zhang L. A review of the green synthesis of ZnO nanoparticles using plant extracts and their prospects for application in antibacterial textiles. Journal of Engineered Fibers and Fabrics. 2021;16.
11. Imade EE, Ajiboye TO, Fadiji AE, Onwudiwe DC, Babalola OO. Green synthesis of zinc oxide nanoparticles using plantain peel extracts and the evaluation of their antibacterial activity. Scientific African. 2022;16:e01152.
12. Rahman F, Majed Patwary MA, Bakar Siddique MA, Bashar MS, Haque MA, Akter B, et al. Green synthesis of zinc oxide nanoparticles using Cocos nucifera leaf extract: characterization, antimicrobial, antioxidant and photocatalytic activity. Royal Society Open Science. 2022;9(11).
13. Sivasankarapillai VS, Krishnamoorthy N, Eldesoky GE, Wabaidur SM, Islam MA, Dhanusuraman R, et al. One-pot green synthesis of ZnO nanoparticles using Scoparia Dulcis plant extract for antimicrobial and antioxidant activities. Applied Nanoscience. 2022;13(9):6093-6103.
14. Mushtaq W, Ishtiaq M, Maqbool M, Mazhar MW, Casini R, Abd-ElGawad AM, et al. Green Synthesis of Zinc Oxide Nanoparticles Using Viscum album Extracts: Unveiling Bioactive Compounds, Antibacterial Potential, and Antioxidant Activities. Plants. 2023;12(11):2130.
15. Al-Askar AA, Hashem AH, Elhussieny NI, Saied E. Green Biosynthesis of Zinc Oxide Nanoparticles Using Pluchea indica Leaf Extract: Antimicrobial and Photocatalytic Activities. Molecules. 2023;28(12):4679.
16. Islam MF, islam S, Miah MAS, Huq AKO, Saha AK, Mou ZJ, et al. Green synthesis of zinc oxide nano particles using Allium cepa L. waste peel extracts and its antioxidant and antibacterial activities. Heliyon. 2024;10(3):e25430.
17. Mohammad s, Wisam Malik A, Mohammed Mohsen S, abbas abbod A. Antibacterial activity of Citrus Aurantium and Myrtus Communis extracts on some pathogenic bacteria. Microbes and Infectious Diseases. 2025;0(0):0-0.
18. Sharma V, Kumar G, Kumar P, Kumar D, Nemiwal M. Green Synthesis of ZnO Nanoparticles from Dysoxylum binectariferum Fruit Extract and Assessment of Antimicrobial Potential. ChemistrySelect. 2024;9(34).
19. Elabbasy MT, El Bayomi RM, Abdelkarim EA, Hafez AE-SE, Othman MS, Ghoniem ME, et al. Antibacterial and Antibiofilm Activity of Green-Synthesized Zinc Oxide Nanoparticles Against Multidrug-Resistant Escherichia coli Isolated from Retail Fish. Molecules. 2025;30(4):768.
20. Assafi MS, Ali FF, Polis RF, Sabaly NJ, Qarani SM. An Epidemiological and Multidrug Resistance Study for E. coli

CC BY

Isolated from Urinary Tract Infection (Three Years of Study). Baghdad Science Journal. 2022;19(1):0007.
21. Jalil MB, Al Atbee MYN. The prevalence of multiple drug resistance Escherichia coli and Klebsiella pneumoniae isolated from patients with urinary tract infections. J Clin Lab Anal. 2022;36(9).
22. Alfuraiji N, Al-Hamami A, Ibrahim M, Rajab HK, Hussain BW. Uropathogenic Escherichia coli virulence characteristics and antimicrobial resistance amongst pediatric urinary tract infections. J Med Life. 2022;15(5):650-654.
23. Eezzeldin HM, Badi S, Yousef BA. The Antibiotic Resistance and Multidrug Resistance Pattern of Uropathogenic Escherichia coli at Soba University Hospital: A Descriptive Retrospective Survey. Sudan Journal of Medical Sciences. 2022;17(1):56-69.
24. Gatya Al-Mayahie SM, Al-Guranie DRdT, Hussein AA, Bachai ZA. Prevalence of common carbapenemase genes and multidrug resistance among uropathogenic Escherichia coli phylogroup B2 isolates from outpatients in Wasit Province/ Iraq. PLoS One. 2022;17(1):e0262984.
25. Mohammed YHI, Alghamdi S, Jabbar B, Marghani D, Beigh S, Abouzied AS, et al. Green Synthesis of Zinc Oxide Nanoparticles Using Cymbopogon citratus Extract and Its Antibacterial Activity. ACS Omega. 2023;8(35):32027-32042.
26. Al-Khaial MQ, Chan SY, Abu-Zurayk RA, Alnairat N. Biosynthesis and Characterization of Zinc Oxide Nanoparticles (ZnO-NPs) Utilizing Banana Peel Extract. Inorganics. 2024;12(4):121.
27. Udayagiri H, Sana SS, Dogiparthi LK, Vadde R, Varma RS, Koduru JR, et al. Phytochemical fabrication of ZnO nanoparticles and their antibacterial and anti-biofilm activity. Sci Rep. 2024;14(1).
28. Dey A, Somaiah S. Green synthesis and characterization of zinc oxide nanoparticles using leaf extract of Thryallis glauca (Cav.) Kuntze and their role as antioxidant and antibacterial. Microscopy Research and Technique. 2022;85(8):2835-2847.
29. Jakinala P, Naik Lavudi H, Angali N, Ganderla S, Inampudi KK, Balaji Andugulapati S, et al. Green synthesis of ZnO-Ag nanocomposite using Stenotaphrum secundatum grass extract: Antibacterial activity and anticancer effect in oral squamous cell carcinoma CAL 27 cells. Inorg Chem Commun. 2023;152:110735.
30. Jiang S, Lin K, Cai M. ZnO Nanomaterials: Current Advancements in Antibacterial Mechanisms and Applications. Frontiers in Chemistry. 2020;8.
31. Vijayakumar A, Mohan R, Jayaprakash P. Green synthesis of ZnO nanoparticles in Zinc chloride:Choline chloride deep eutectic solvent-characterization antibacterial and antioxidant agents. J Indian Chem Soc. 2024;101(11):101375.
32. Gudkov SV, Burmistrov DE, Serov DA, Rebezov MB, Semenova AA, Lisitsyn AB. A Mini Review of Antibacterial Properties of ZnO Nanoparticles. Frontiers in Physics. 2021;9.
33. Agrawal A, Sharma R, Sharma A, Gurjar KC, Kumar S, Chatterjee S, et al. Antibacterial and antibiofilm efficacy of green synthesized ZnO nanoparticles using Saraca asoca leaves. Environmental Science and Pollution Research. 2023;30(36):86328-86337.
34. Abu-Gharbia MA, El-Sayed MF, Salem JM, Abd-Elsamei WM, Al-Arabi G. Antibacterial impact of biosynthesized zinc oxide nanoparticles on uropathogenic Escherichia coli and in vivo assessment of physiological and histological alterations. Sci Rep. 2025;15(1).
35. Elekhnawy E, Almurshedi AS, Abdelkader DH, El-Masry TA, Aldosari BN, El-Bouseary MM, et al. Green synthesised zinc oxide nanoparticles reveal potent in vivo and in vitro antibacterial efficacy against Proteus mirabilis isolates. Int J Pharm. 2023;642:123111.
36. Hasan J, Khalaf Z, Jasim S. Antimicrobial Activity Zinc Oxide ZnO Nanoparticles Against Biofilm Formation of Uropathogenic E. coli. 5th International Conference on Biomedical and Health Sciences: Cihan University-Erbil; 2024. p. 257-261.
37. Shakerdarabad R, Mohabatkar H, Behbahani M, Dini G. Antibiofilm and antibacterial activities of green synthesized ZnO nanoparticles against Erwinia amylovora and Pseudomonas syringae pv. Syringae: in vitro and in silico investigations. Microb Pathog. 2024;196:107011.
38. Abdelghafar A, Yousef N, Askoura M. Zinc oxide nanoparticles reduce biofilm formation, synergize antibiotics action and attenuate Staphylococcus aureus virulence in host; an important message to clinicians. BMC Microbiol. 2022;22(1).
39. Zhu X, Wang J, Cai L, Wu Y, Ji M, Jiang H, et al. Dissection of the antibacterial mechanism of zinc oxide nanoparticles with manipulable nanoscale morphologies. J Hazard Mater. 2022;430:128436.

CC BY